

# Stable Small Quantum Dots for Synaptic Receptor Tracking on Live Neurons\*\*

En Cai, Pinghua Ge, Sang Hak Lee, Okunola Jeyifous, Yong Wang, Yanxin Liu, Katie M. Wilson, Sung Jun Lim, Michelle A. Baird, John E. Stone, Kwan Young Lee, Michael W. Davidson, Hee Jung Chung, Klaus Schulten, Andrew M. Smith, William N. Green, and Paul R. Selvin\*

**Abstract:** We developed a coating method to produce functionalized small quantum dots (sQDs), about 9 nm in diameter, that were stable for over a month. We made sQDs in four emission wavelengths, from 527 to 655 nm and with different functional groups. AMPA receptors on live neurons were labeled with sQDs and postsynaptic density proteins were visualized with super-resolution microscopy. Their diffusion behavior indicates that sQDs access the synaptic clefts significantly more often than commercial QDs.

Quantum dots (QDs), made of semiconductor nanocrystals, are highly advantageous in fluorescence applications because of their brightness and high photostability.<sup>[1]</sup> In particular, they are widely used in single-molecule experiments such as single-particle tracking in living cells.<sup>[2–5]</sup> However, their large diameters, typically around 15–35 nm for commercially available QDs,<sup>[6]</sup> significantly reduce their access to spatially confined cellular environments such as cell junctions.<sup>[2]</sup> There have been attempts to make smaller QDs, generally with diameters on the order of 10 nm.<sup>[7–9]</sup> However, small quantum dots usually suffer either from chemical instability or poor labeling specificity.<sup>[2]</sup>

Achieving specific labeling with small QDs is particularly challenging on neurons, especially when labeling proteins in synaptic clefts, the 30 nm thin spaces separating two neurons at synapses (Figure 1a). The commercially available QDs (we refer to them as big QDs, or bQDs), have been successfully used to label neurons,<sup>[10,11]</sup> although the majority of bQDs (typically 70–90 %) label extra-synaptic sites, rather than sites within synapses, because of their large sizes.<sup>[7,11]</sup>

The large size of bQDs primarily results from their passivating surface coating and attached biomolecules. The quantum dot crystal, often made of a cadmium selenide (CdSe) core with a zinc sulfide (ZnS) shell, is typically 2–7 nm in diameter, and is coated with selected groups of chemicals for dispersion and stabilization in water.<sup>[12]</sup> Commercial QDs are usually coated with thick polymer layers that attach to many bioaffinity groups (e.g. streptavidins), together resulting in a large size. Other coating methods have been developed to reduce the size of QDs.<sup>[5,7,8,13–17]</sup> In particular, Howarth et al. reported the use of DHLA-PEG derivatives for coating CdSe/ZnCdS QDs which reduced the size of QDs to 11 nm with stability at 37 °C for more than 4 h.<sup>[7]</sup> The reduced-sized QDs were reported to have better accessibility to the synaptic

[\*] Dr. E. Cai,<sup>[‡]</sup> Dr. P. Ge,<sup>[‡]</sup> Dr. S. H. Lee, Dr. O. Jeyifous, Dr. Y. Wang, Dr. Y. Liu, Prof. Dr. K. Schulten, Prof. Dr. P. R. Selvin  
Department of Physics and Center for the Physics of Living Cells  
University of Illinois at Urbana-Champaign  
1110 W Green St., Urbana, IL 61801 (USA)  
E-mail: selvin@illinois.edu

Dr. O. Jeyifous, Prof. Dr. W. N. Green  
Department of Neurobiology, University of Chicago  
Chicago, IL (USA)

Dr. Y. Liu, J. E. Stone, Prof. Dr. K. Schulten  
Beckman Institute  
University of Illinois at Urbana-Champaign, Urbana, IL (USA)

Dr. K. M. Wilson  
Department of Structural and Chemical Biology and  
Institute of Integrative Biology, University of Liverpool  
Liverpool (UK)

Dr. S. J. Lim, Prof. Dr. A. M. Smith  
Department of Bioengineering  
University of Illinois at Urbana-Champaign, Urbana, IL (USA)

M. A. Baird, M. W. Davidson  
The National High Magnetic Field Laboratory and  
Department of Biological Science  
The Florida State University, Tallahassee, FL (USA)

Dr. K. Y. Lee, Prof. Dr. H. J. Chung  
Department of Molecular and Integrative Physiology  
University of Illinois at Urbana-Champaign  
Urbana, IL (USA)

Prof. Dr. K. Schulten, Prof. Dr. P. R. Selvin  
Center for Biophysics and Computational Biology  
University of Illinois at Urbana-Champaign  
Urbana, IL (USA)

Prof. Dr. W. N. Green, Prof. Dr. P. R. Selvin  
Marine Biological Laboratory  
Woods Hole, MA (USA)

[‡] These authors contributed equally to this work.

[\*\*] This work was supported by NSF grants MCB 1216342, DBI 1063188 (to P.R.S.) and PHY 1430124 (to P.R.S. and K.S.) and NIH grant R21 NS087413 (to P.R.S.). We would also like to acknowledge NIH grant 5P41GM104601 to K.S.. A.M.S. acknowledges the NIH grant R00 CA153914. W.N.G. acknowledges the NIH grants R01 NS043782 and R01 DA035430, and W.N.G. and P.R.S. acknowledge summer fellowships from Marine Biological Laboratory in 2010 and 2011. We thank P. Dionne and P. De Koninck for sharing their constructs and labeling protocol with us. We thank K. W. Teng for technical assistance and D. G. Fernig for initial consultation and advice.



Supporting information for this article is available on the WWW under <http://dx.doi.org/10.1002/anie.201405735>.

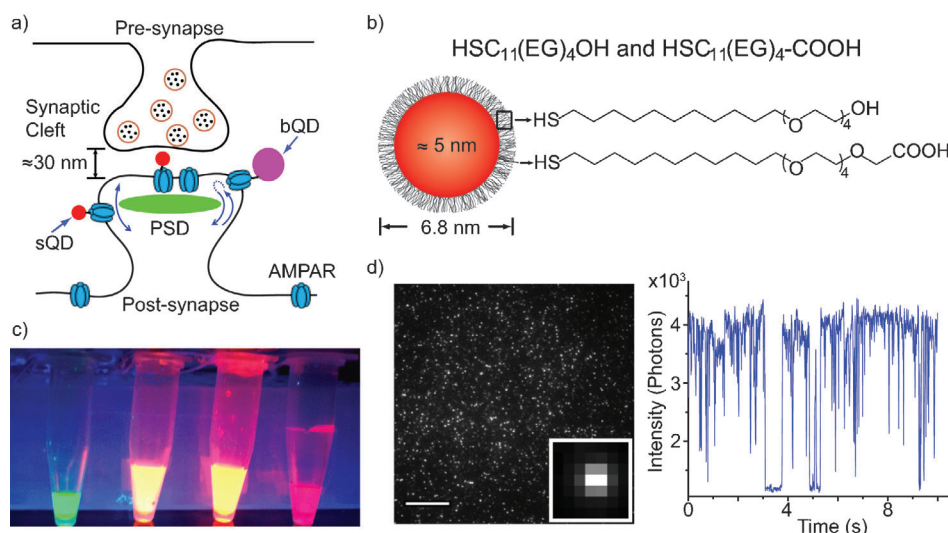


**Figure 1.** Characterizations of small quantum dots. a) Schematic diagram of the synaptic region with AMPA receptors (AMPA) labeled with sQDs and commercial QDs. b) Schematic diagram of the sQD. sQDs are coated with PEGylated alkanethiol ligands by self-assembly monolayer. c) Fluorescence of sQDs with emission 527, 615, 620, and 655 nm in PBS (pH 7.3) under UV illumination. All sQDs are soluble and mono-dispersed in PBS. d) Single molecule fluorescent image of sQD-620-streptavidin bound to biotins fixed on a coverslip. Fluorescent intensity of sQD-620 over time is shown at right. Blinking behavior is observed. Scale bar: 15  $\mu\text{m}$ .

cleft compared to bQDs. However, problems with chemical stability of the coating and variability of the QD cores ultimately led to an abandonment of this procedure.

Here we report that coating with a thin, but stable, ligand layer over the usual CdSe/ZnS QD cores, allows for compact probes with substantially improved access to neuronal synapses. We use a self-assembled monolayer<sup>[18]</sup> of hydrophilic ligands with the structure  $\text{HS}-(\text{CH}_2)_{11}-(\text{EG})_4-\text{OH}/\text{COOH}$  (EG: ethylene glycol) (Figure 1b; and Figure S1 in the Supporting Information). Both the ligand structure and coating method are critical. The undecanethiol termination provides a hydrophobic attachment to the nanoparticle surface that resists desorption, and unlike bulkier DHLA-based ligands, packs densely on the QD surface. The short  $\text{EG}_4$  chain provides hydrophilicity for stable aqueous dispersion. The key parameter in the coating procedure is the use of elevated temperature without oxygen (60 °C, 4 h,  $\text{N}_2$ ) to drive replacement of the native hydrophobic ligands with a dense layer of the new ligands. The ligand monolayer makes them stable in water (over 1 month) and brightly fluorescent (28% quantum yield). They are also resistant to non-specific binding to biomolecules, across a wide panel of QD crystal sizes (3.2–8 nm), sources (NN-labs, Invitrogen, and laboratory-made), and batches, yielding a broad spectrum of fluorescence wavelengths (Figure 1c). For the sake of simplicity, we call them small QDs (sQDs).

Streptavidin (SA) was conjugated to the COOH-functionalized sQDs by a straightforward EDC coupling method. Individual sQDs were bound to biotin molecules on a PEGylated coverslip, and fluorescent blinking was observed (Figure 1d). The average intensity was approximately 1/3 that of the bQDs (see the Experimental Section in the Supporting Information). By only using a small number of COOH groups

(10%) in the ligand layer, the rest being OH groups, non-specific labeling is minimized and only a small number of bioaffinity molecules can attach to maintain a small particle size. Dynamic light scattering (DLS) measurements showed that the hydrodynamic diameter of the SA-functionalized sQD-620 was  $8.9 \pm 0.2$  nm (Figure S2a). These functionalized sQDs are stable for over one month at 4 °C (Figure S2b–e).

A major limitation in labeling live neurons with sQDs is non-specific interactions, between sQDs and neurons, or between sQDs and substrate, particularly positively charged polylysine that is often used to attach neurons onto the coverslip. To test the binding specificity of our sQDs, we co-transfected neurons with the postsy-

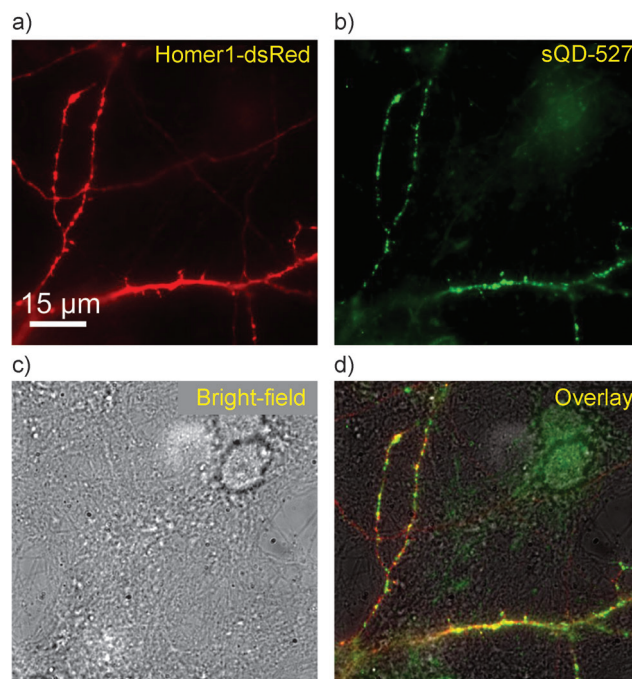


**Figure 2.** Specific labeling of sQDs on biotinylated AMPA receptors expressed in live neurons. Neurons were co-transfected with post-synaptic Homer1-dsRed and biotinylated GluA2-AP (see text). a) Fluorescent image of a neuron expressing Homer1-dsRed (red; scale bar = 15  $\mu\text{m}$ ). b) Fluorescent image of 527 nm emitting sQD-streptavidin bound to biotinylated GluA2-AP subunit of the AMPAR (green). c) Bright-field image of the same region as in a) and b) show that the field of view is covered with neurons. d) Overlay of Homer1-dsRed, sQD-labeled AMPARs, and brightfield image (a, b, c) shows that the labeling was highly specific to the transfected neuron. Very few sQDs were found on untransfected neurons or on the coverslip.

naptic density (PSD) protein Homer1<sup>[12]</sup> and the AMPA receptor (AMPA) subunit GluA2.<sup>[20]</sup> Homer1 was fused with a fluorescent protein (FP), dsRed, for the visualization of the PSDs. GluA2 was modified by genetically attaching a 15-mer amino acid acceptor peptide (AP) tag at the extracellular domain,<sup>[21]</sup> which was biotinylated by co-transfected biotin ligase (BirA) in the endoplasmic reticulum.<sup>[21,22]</sup> Biotinylation of GluA2-AP allowed labeling by SA-sQDs on the surface of transfected neurons. As shown in Figure 2, overlap between Homer1 and AMPARs was observed; minimum binding of the SA-sQDs was found on untransfected neurons. The high-labeling specificity on neurons was also achieved with other sQDs at different emission wavelengths (Figure S3). In summary, sQDs, like bQDs, specifically labeled biotinylated AMPARs, allowing for the tracking of single AMPARs.

We next tracked AMPARs labeled with either sQDs or bQDs and compared their accessibility to synaptic clefts and compared their diffusion patterns. To improve the resolution of PSDs, we fused Homer1 with the photoactivatable FP (paFP) mGeos-M,<sup>[23]</sup> which emits in the GFP channel when activated by near-UV (405 nm) light. Using photoactivated localization microscopy (PALM),<sup>[24,25]</sup> the mGeos-M molecules can be localized with precision of 14 nm in the *x,y* plane.<sup>[23]</sup> The sQDs for AMPAR labeling were then chosen with an emission wavelength different than the paFP—in this case, at 620 nm—and therefore could be detected separately using 3-D single-particle tracking by a modified form of fluorescence imaging with one nanometer accuracy (FIONA).<sup>[26,27]</sup> By combining single-particle tracking and PALM we were able to observe 3-D diffusion of QD-labeled AMPARs at synapses with high spatial resolution (Figure 3).

We observed different diffusion behavior for the sQD-labeled and bQD-labeled AMPARs. AMPARs labeled with bQDs diffuse rapidly along dendrites, often moving between synapses (Figure 3a, and movie S1). The majority (79%) of the bQD-AMPA receptors travelled distances larger than 1  $\mu\text{m}$  in either *x*-, *y*-, or *z*-directions (Figure 3b). We further calculated the diffusion coefficients of the bQD-AMPA receptors and found that only 11% of the receptors were

immobile (diffusion coefficient  $D < 0.01 \mu\text{m}^2 \text{s}^{-1}$ ), 29% of the receptors were slowly diffusing ( $0.01 \mu\text{m}^2 \text{s}^{-1} < D < 0.1 \mu\text{m}^2 \text{s}^{-1}$ ), and the majority of receptors (60%) were rapidly diffusing ( $D > 0.1 \mu\text{m}^2 \text{s}^{-1}$ ) (Figure 3c). In contrast, the sQD-AMPA receptors tended to diffuse within a confined range. As shown in Figure 3d and movie S2, a population of the sQD-AMPA receptors were located within PSDs, with another population labeled specifically at other regions along the dendrites lacking fluorescent Homer1 molecules. Whether these other regions are synapses, or other subcellular domains, was not determined. Specifically, only a small fraction (18%) of the sQD-AMPA receptors travelled large distances along the dendrites, with a trajectory range greater than 1  $\mu\text{m}$  (Figure 3e). In particular, 37% of sQD-AMPA receptors were immobile, 59% showed slow diffusion, and only 4% were fast diffusing (Figure 3f). In summary, 82% of the sQD-AMPA receptors are confined to diffuse over a limited ( $< 1 \mu\text{m}$ ) space, while only 21% of the bQD-AMPA receptors are limited in their diffusion.

The two possibilities that can explain the results of slower diffusion of the sQDs compared to the bQDs, are that the

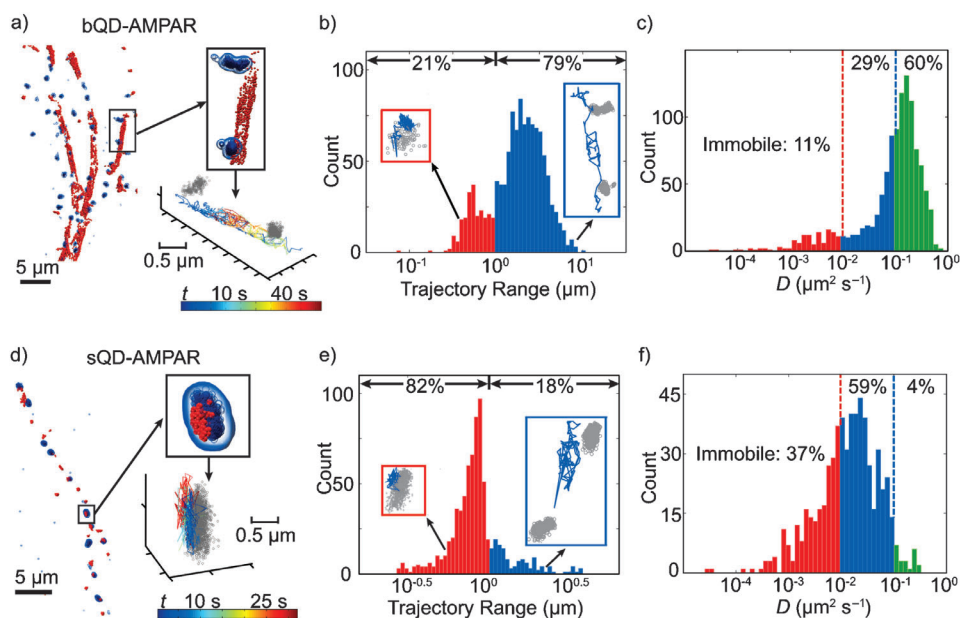


**Figure 3.** Different diffusion behavior of sQD-AMPA receptors and commercial QD-AMPA receptors. a) Images of AMPARs labeled with commercial QDs (bQDs) diffusing between synapses. The blue clusters depict localizations of postsynaptic marker Homer1-mGeos-M, and the red dots are localizations of bQD-labeled receptors at different time points on trajectories. One region is enlarged to show the AMPAR diffusing along the dendrite between two synapses. The same region is shown at the bottom with trajectories colored by time. Gray clusters indicate the synapses. b) Histogram of “trajectory range” of AMPARs labeled with commercial QDs (bQDs). The trajectory range is the maximum distance of the trajectory in either the *x*, *y*, or *z* dimension. It quantifies the spatial confinement of AMPAR diffusion. The fraction of trajectories with range  $< 1 \mu\text{m}$  are 21%, shown as red bar. The fraction of trajectories with range  $> 1 \mu\text{m}$  are shown as blue bar. Insets are example trajectories (blue) around the synapse (gray). c) Histograms of diffusion coefficients of AMPARs labeled with bQD. For AMPARs labeled with bQDs, only 11% of the receptors are immobile ( $D < 0.01 \mu\text{m}^2 \text{s}^{-1}$ , red bars), and 60% are diffusing rapidly ( $D > 0.1 \mu\text{m}^2 \text{s}^{-1}$ , green bars), with 29% having intermediate diffusion coefficients (blue bars). d)–f) Same scheme as in a)–c), except AMPARs are labeled with sQDs, show that sQD-labeled AMPARs are primarily localized around synapses. For the sQDs-labeled AMPARs, 37% of receptors are immobile, and only 4% are diffusing fast, with 59% having intermediate diffusion coefficients. A comparison of b)–c) and e)–f) clearly shows the labeling difference between the sQDs and the bQDs. All trajectories in each histogram were collected from four dendritic regions. Images a) and d) were partially rendered using the QuickSurf representation in VMD 1.9.2.<sup>[36]</sup>



surface chemistry is somehow different between the two, or that the sQDs are hindered (or, in the extreme case, immobilized), by the interaction with the PSDs more than the bQDs.

The difference in the diffusion behavior between sQDs and bQDs labeled AMPARs on neurons is not due to the different surface chemistry of QDs. We perform the same experiments and analysis above on the surface of HEK 293 cells, where no spatially confined domains exist, such as synapses. On HEK cells, we observed similar diffusion behavior between bQDs and sQDs (Figure S4). The majority of AMPARs (87 % with bQDs and 73 % with sQDs) were fast diffusing ( $D > 0.1 \mu\text{m}^2\text{s}^{-1}$ ). Therefore, the reduced ranges and diffusion coefficients of sQD-AMPARs on neurons result from the reduced QD size.

Synaptic receptors such as AMPARs are known to diffuse slower in the postsynaptic sites than in extrasynaptic site because of higher membrane viscosity in the postsynapse,<sup>[28]</sup> as well as receptor interaction with scaffold proteins in the PSD.<sup>[10,29]</sup> From our data, it appears that the constrained diffusion of the sQDs is because they have greater access than the bQDs to the AMPARs in the PSDs. This further suggests that sQD-labeled AMPARs in the synapse move in a confined space, resulting in a higher population of slow diffusion than the bQD-labeled AMPARs. To test this possibility, we examined the trajectories of AMPARs within 2  $\mu\text{m}$  radius of the locations of Homer1 and found that 37 % of sQD trajectories were synaptic, compared to 10 % of bQD trajectories (Figure S5). Our results are consistent with previous reports of an increased number of sQD (about 11 nm) labeled AMPARs at synapses, compared to AMPARs labeled with bQDs.<sup>[7,11]</sup> Despite differences in detailed protocol and analysis algorithm used, Howarth et al. estimated that 24 % of bQDs and 46 % of sQDs co-localized at synapses;<sup>[7]</sup> Groc et al. using a Cy3-antibody estimated 9.4 % at synapses, 20.3 % using Cy3-bungarotoxin and 5.4 % using a bQD-antibody to a GFP.<sup>[11]</sup>

We note that Farlow et al.<sup>[30]</sup> developed a monovalent quantum dot (about 12 nm in diameter) by steric exclusion. They used a functionalized oligonucleotide to wrap the QDs, making it monovalent and therefore reduce the possibility of cross-linking target proteins. However, it carries large amount of negative charges and would cause significant non-specific binding to the polylysine coated coverslip when labeling neurons.

It is possible that, in our experiments, a streptavidin (with four biotin binding sites), or multiple streptavidin per QD can induce cross-linking between AMPARs, and therefore reduce the AMPAR mobility. However, our data indicates this is unlikely. The reason is that the diffusion constant of AMPARs labeled with bQD-SA are similar to that labeled with organic fluorescent dye conjugated antibodies. (Large-scale cross-linking is unlikely—though still possible—to be induced by dye-labeled antibodies). In particular, we find that mobile AMPAR (GluA2 subunit) labeled with bQD-SA has a median diffusion constant of  $0.15 \mu\text{m}^2\text{s}^{-1}$ , in rough agreement with AMPAR diffusion measured with Cy3-antibodies by Groc et al. (median  $0.08 \mu\text{m}^2\text{s}^{-1}$  for mobile GluA2),<sup>[31]</sup> and with ATTO647N-anti-GluA2 by Giannone et al. (median

$0.10 \mu\text{m}^2\text{s}^{-1}$ ).<sup>[32]</sup> Furthermore, the number of SA per sQD is even less than with bQD, and therefore, it is unlikely that sQD induces cross-linking. Finally, we also tested AMPAR diffusion on the cytoplasmic side of HEK cells (Figure S4). Here the diffusion of AMPARs measured by bQD and sQD are similar, which also support the fact that sQDs do not induce AMPAR-cross-linking.

Nevertheless, to further reduce the chances of cross-linking, one could separate out sQD with single copy of SA by gel electrophoreses,<sup>[7,16,33]</sup> or one could reduce the percentage of -COOH in the coating (e.g. from 10 % to approximately 2.5 %), resulting in fewer SAs per sQD. In addition, it is straightforward to functionalize sQD with other biomolecules, such as biotin or GBP<sup>[34]</sup> (a 13 kD nanobody against GFP) instead of SA (Figure S6), which could be used to produce monovalent sQD. It is also possible to functionalize sQD with a PEGylated  $\text{O}_6$ -alkylguanine derivative to label fusion proteins with a SNAP tag (19.4 kD).<sup>[35]</sup> By making the sQD monofunctional and using smaller molecules as functional groups, the effective size of sQD can be further reduced, making it a better fluorescent probe to function in a crowded cellular environment.

In conclusion, we have developed a simple method to coat quantum dot cores, producing a smaller streptavidin-functionalized sQDs ( $8.9 \pm 0.2$  nm in diameter) than commercially available QDs (15–35 nm). Our sQDs are also chemically more stable than the previous generation of sQDs.<sup>[7]</sup> These sQDs enable specific labeling of AMPARs and allowed much greater access to the synaptic region than bQDs. Combined with three-dimensional super-resolution imaging, which can localize pre- and post-synaptic region, the biomolecules labeled with sQDs can be investigated by single particle tracking. Their application is not limited to the synapse but extends to any subcellular structures, particularly confined spaces or crowded spaces in cells where small fluorescent probes with tremendous photostability are advantageous.

Received: May 28, 2014

Revised: August 13, 2014

Published online: September 26, 2014

**Keywords:** AMPA receptors · fluorescent probes · quantum dots · single-molecule studies

- [1] X. Michalet, F. F. Pinaud, L. A. Bentolila, J. M. Tsay, S. Dooze, J. J. Li, G. Sundaresan, A. M. Wu, S. S. Gambhir, S. Weiss, *Science* **2005**, 307, 538–544.
- [2] F. Pinaud, S. Clarke, A. Sittner, M. Dahan, *Nat. Methods* **2010**, 7, 275–285.
- [3] M. M. Echarte, L. Bruno, D. J. Arndt-Jovin, T. M. Jovin, L. I. Pietrasanta, *FEBS Lett.* **2007**, 581, 2905–2913.
- [4] D. S. Lidke, K. A. Lidke, B. Rieger, T. M. Jovin, D. J. Arndt-Jovin, *J. Cell Biol.* **2005**, 170, 619–626.
- [5] C. You, S. Wilmes, O. Beutel, S. Löchte, Y. Podoplelowa, F. Roder, C. Richter, T. Seine, D. Schaible, G. Uzé, et al., *Angew. Chem. Int. Ed.* **2010**, 49, 4108–4112; *Angew. Chem.* **2010**, 122, 4202–4206.
- [6] R. A. Sperling, T. Liedl, S. Duhr, S. Kudera, M. Zanella, C.-A. J. Lin, W. H. Chang, D. Braun, W. J. Parak, *J. Phys. Chem. C* **2007**, 111, 11552–11559.

- [7] M. Howarth, W. Liu, S. Puthenveetil, Y. Zheng, L. F. Marshall, M. M. Schmidt, K. D. Wittrup, M. G. Bawendi, A. Y. Ting, *Nat. Methods* **2008**, *5*, 397–399.
- [8] W. Liu, M. Howarth, A. B. Greytak, Y. Zheng, D. G. Nocera, A. Y. Ting, M. G. Bawendi, *J. Am. Chem. Soc.* **2008**, *130*, 1274–1284.
- [9] N. Zhan, G. Palui, M. Safi, X. Ji, H. Mattoussi, *J. Am. Chem. Soc.* **2013**, *135*, 13786–13795.
- [10] M. Dahan, S. Lévi, C. Luccardini, P. Rostaing, B. Riveau, A. Triller, *Science* **2003**, *302*, 442–445.
- [11] L. Groc, M. Lafourcade, M. Heine, M. Renner, V. Racine, J.-B. Sibarita, B. Lounis, D. Choquet, L. Cognet, *J. Neurosci.* **2007**, *27*, 12433–12437.
- [12] R. Gill, M. Zayats, I. Willner, *Angew. Chem. Int. Ed.* **2008**, *47*, 7602–7625; *Angew. Chem.* **2008**, *120*, 7714–7736.
- [13] D. G. Fernig, L. Duchesne, *Nanoparticle Conjugates* US20110165647A1, **2011**.
- [14] B. A. Kairdolf, A. M. Smith, T. H. Stokes, M. D. Wang, A. N. Young, S. Nie, *Annu. Rev. Anal. Chem.* **2013**, *6*, 143–162.
- [15] W. Liu, A. B. Greytak, J. Lee, C. R. Wong, J. Park, L. F. Marshall, W. Jiang, P. N. Curtin, A. Y. Ting, D. G. Nocera, et al., *J. Am. Chem. Soc.* **2010**, *132*, 472–483.
- [16] S. Clarke, F. Pinaud, O. Beutel, C. You, J. Piehler, M. Dahan, *Nano Lett.* **2010**, *10*, 2147–2154.
- [17] F. Pinaud, D. King, H.-P. Moore, S. Weiss, *J. Am. Chem. Soc.* **2004**, *126*, 6115–6123.
- [18] L. Duchesne, D. Gentili, M. Comes-Franchini, D. G. Fernig, *Langmuir* **2008**, *24*, 13572–13580.
- [19] Y. Sugiyama, I. Kawabata, K. Sobue, S. Okabe, *Nat. Methods* **2005**, *2*, 677–684.
- [20] M. Hollmann, S. Heinemann, *Annu. Rev. Neurosci.* **1994**, *17*, 31–108.
- [21] M. Howarth, K. Takao, Y. Hayashi, A. Y. Ting, *Proc. Natl. Acad. Sci. USA* **2005**, *102*, 7583–7588.
- [22] M. Howarth, A. Y. Ting, *Nat. Protoc.* **2008**, *3*, 534–545.
- [23] H. Chang, M. Zhang, W. Ji, J. Chen, Y. Zhang, B. Liu, J. Lu, J. Zhang, P. Xu, T. Xu, *Proc. Natl. Acad. Sci. USA* **2012**, *109*, 4455–4460.
- [24] E. Betzig, G. H. Patterson, R. Sougrat, O. W. Lindwasser, S. Olenych, J. S. Bonifacino, M. W. Davidson, J. Lippincott-Schwartz, H. F. Hess, *Science* **2006**, *313*, 1642–1645.
- [25] B. Huang, W. Wang, M. Bates, X. Zhuang, *Science* **2008**, *319*, 810–813.
- [26] A. Yildiz, J. N. Forkey, S. A. McKinney, T. Ha, Y. E. Goldman, P. R. Selvin, *Science* **2003**, *300*, 2061–2065.
- [27] R. Henriques, M. Lelek, E. F. Fornasiero, F. Valtorta, C. Zimmer, M. M. Mhlana, *Nat. Methods* **2010**, *7*, 339–340.
- [28] M. Renner, D. Choquet, A. Triller, *J. Neurosci.* **2009**, *29*, 2926–2937.
- [29] K. Czöndör, M. Mondin, M. Garcia, M. Heine, R. Frischknecht, D. Choquet, J.-B. Sibarita, O. R. Thoumine, *Proc. Natl. Acad. Sci.* **2012**, *109*, 3522–3527.
- [30] J. Farlow, D. Seo, K. E. Broaders, M. J. Taylor, Z. J. Gartner, Y. Jun, *Nat. Methods* **2013**, *10*, 1203–1205.
- [31] L. Groc, M. Heine, L. Cognet, K. Brickley, F. A. Stephenson, B. Lounis, D. Choquet, *Nat. Neurosci.* **2004**, *7*, 695–696.
- [32] G. Giannone, E. Hosy, F. Levet, A. Constals, K. Schulze, A. I. Sobolevsky, M. P. Rosconi, E. Gouaux, R. Tampe, D. Choquet, et al., *Biophys. J.* **2010**, *99*, 1303–1310.
- [33] M. S. Itano, A. K. Neumann, P. Liu, F. Zhang, E. Gratton, W. J. Parak, N. L. Thompson, K. Jacobson, *Biophys. J.* **2011**, *100*, 2662–2670.
- [34] U. Rothbauer, K. Zolghadr, S. Muyldermans, A. Schepers, M. C. Cardoso, H. Leonhardt, *Mol. Cell. Proteomics* **2008**, *7*, 282–289.
- [35] M. Colombo, S. Mazzucchelli, J. M. Montenegro, E. Galbiati, F. Corsi, W. J. Parak, D. Prospero, *Small* **2012**, *8*, 1492–1497.
- [36] W. Humphrey, A. Dalke, K. Schulten, *J. Mol. Graph.* **1996**, *14*, 33–38.